

Electronic Supplementary Information

Boron-manganese-carbon nanocomposites
synthesized from CO₂ for electrode applications in
both supercapacitor and fuel cell

Yeeun Kim^a, Wonhee Lee^{a,b}, Gi Mihn Kim^a and Jae W. Lee^{a*}

^a Department of Chemical and Biomolecular Engineering, Korea

Advanced Institute of Science and Technology (KAIST), 291

Daehak-ro, Yuseong-gu, Daejeon 305-701, Republic of Korea ^b

Climate Change Research Division, Korea Institute of Energy

Research (KIER), 152 Gajeong-ro, Yuseong-gu, Daejeon 34129,

Republic of Korea

S.1 The conversion of potentials against a reversible hydrogen electrode (RHE)

To compare with other studies, the measured potential with respect to Ag/AgCl as a reference electrode can be converted against reversible hydrogen electrode (RHE) by following equation (S1):

$$E_{RHE} = E_{Ag/AgCl} + 0.059 pH + E_{Ag/AgCl}^{\circ} \quad (S1)$$

Where pH is 13.6 in 1.0 M NaOH, and $E_{Ag/AgCl}^{\circ}$ is 0.1976 V at 25 °C.¹

S.2 The RRDE measurement

The electron transfer number (n) and hydrogen peroxide yield ($x_{H_2O_2}$) for ORR were determined by using RRDE measurement data with equations (S2) and (S3).

$$n = \frac{4I_D}{I_D + I_R/N} \quad (S2)$$

$$x_{H_2O_2} = \frac{2I_R/N}{I_D + I_R/N} \quad (S3)$$

Where I_D is the disk current (A), I_R is the ring current (A), and N is the RRDE collection efficiency, which was 0.424 herein ².

S.3 The specific capacitance equation

The specific capacitance was calculated from the galvanostatic charge/discharge curves using equation (S4).

$$C_{GCD} = \frac{I\Delta t}{m\Delta V} \quad (\text{S4})$$

where I is the constant current density, Δt is the discharging time, m is the mass of only BPCMO material used for the working electrode, and ΔV is the discharging voltage change³.

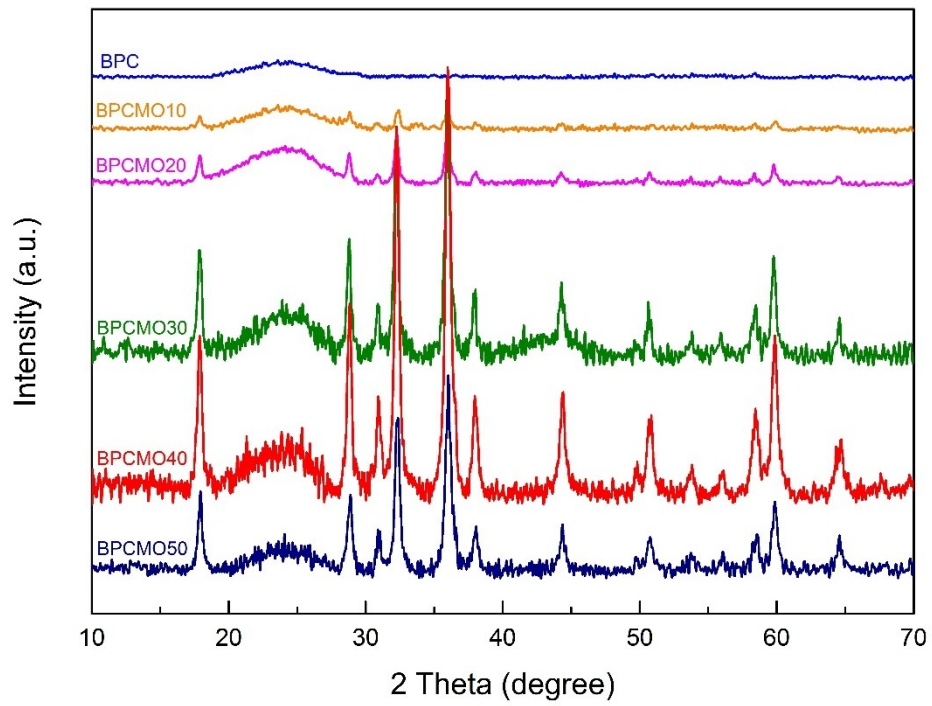


Fig. S1 XRD spectra of BPC and BPCMOs.

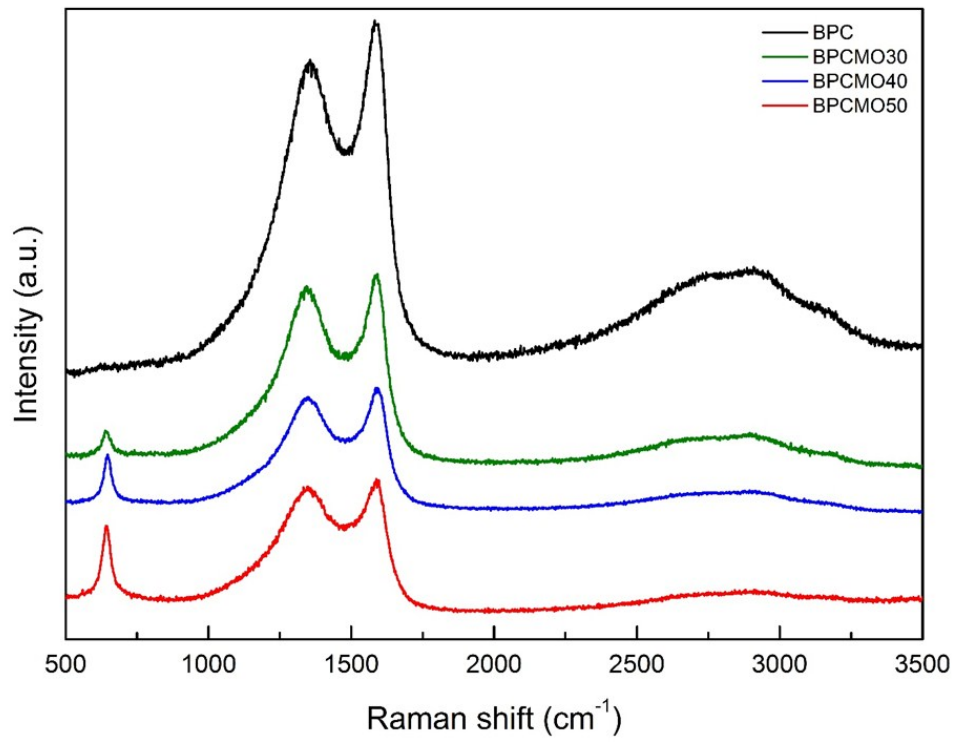


Fig. S2 Raman spectra of BPC and BPCMOs.

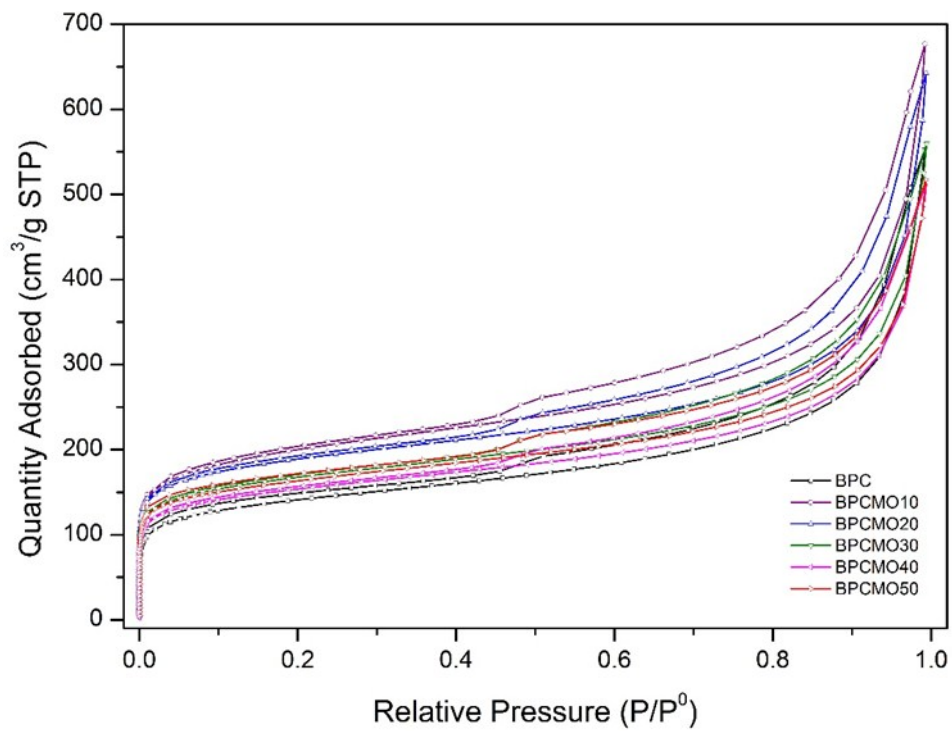


Fig. S3 Nitrogen adsorption isotherms of BPC series.

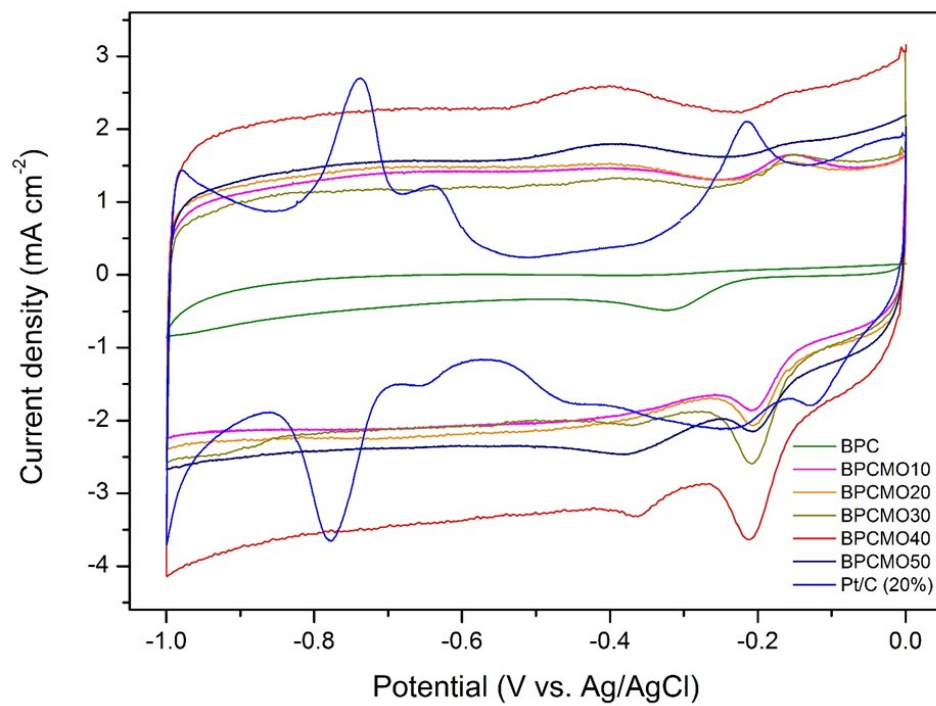


Fig. S4 CV of Pt/C (20wt%) and BPCMO series (scan rate = 50 mVsec⁻¹).

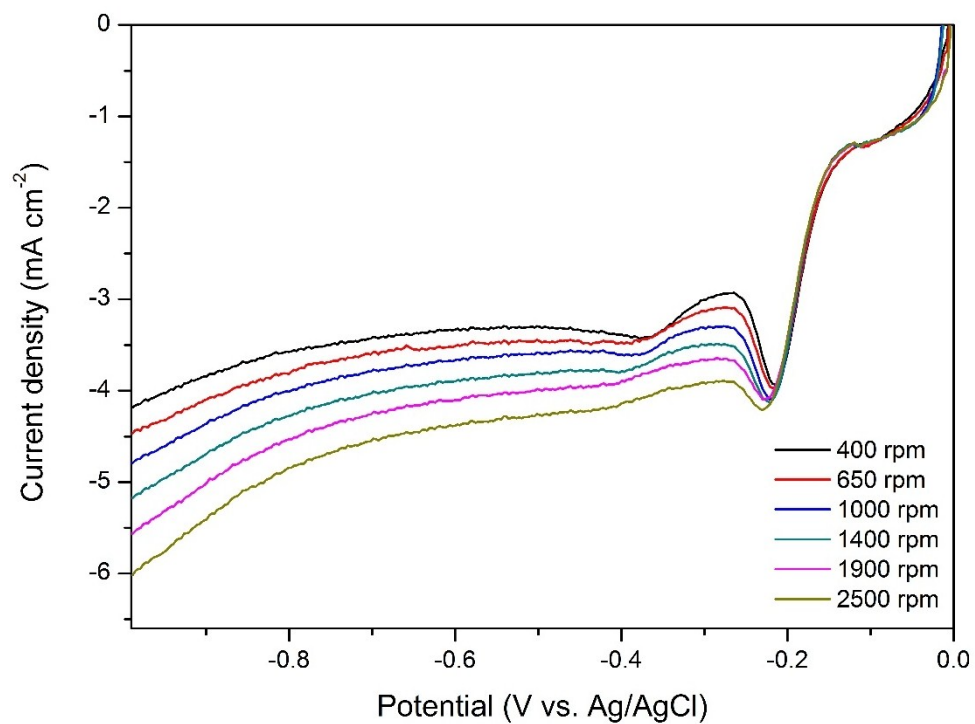


Fig. S5 LSV of BPCMO40 according to different rotation speeds (scan rate = 50 mVsec⁻¹).

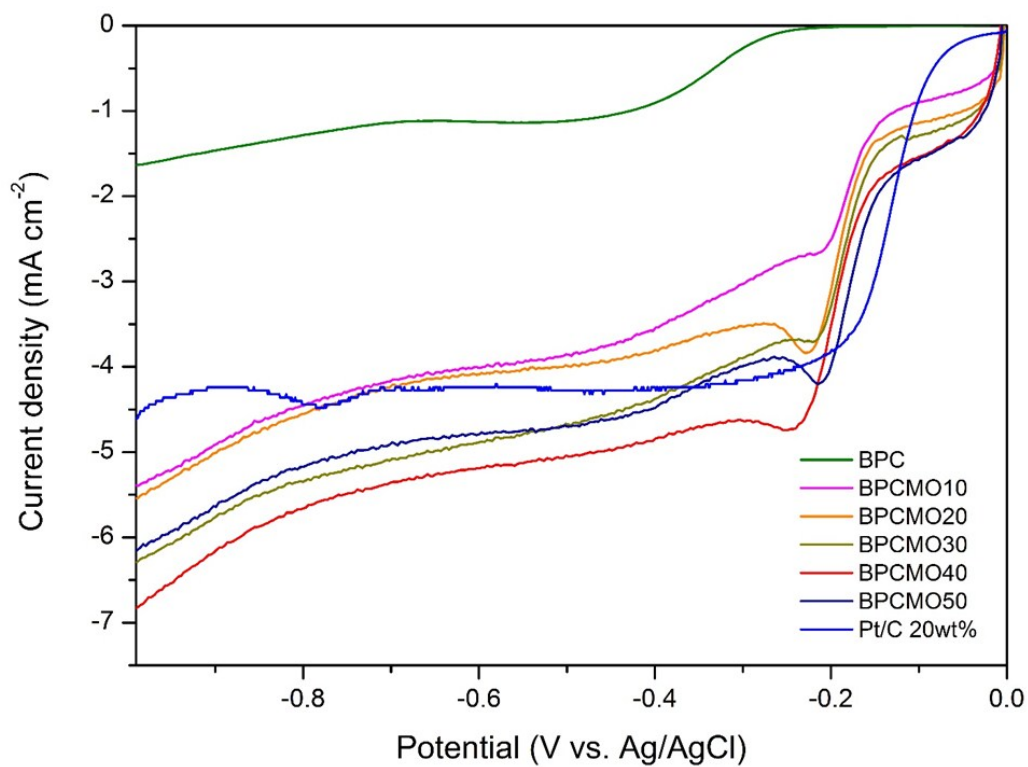


Fig. S6 LSV of BPCMO series at 2500 rpm and at a scan rate of 50 mVsec⁻¹.

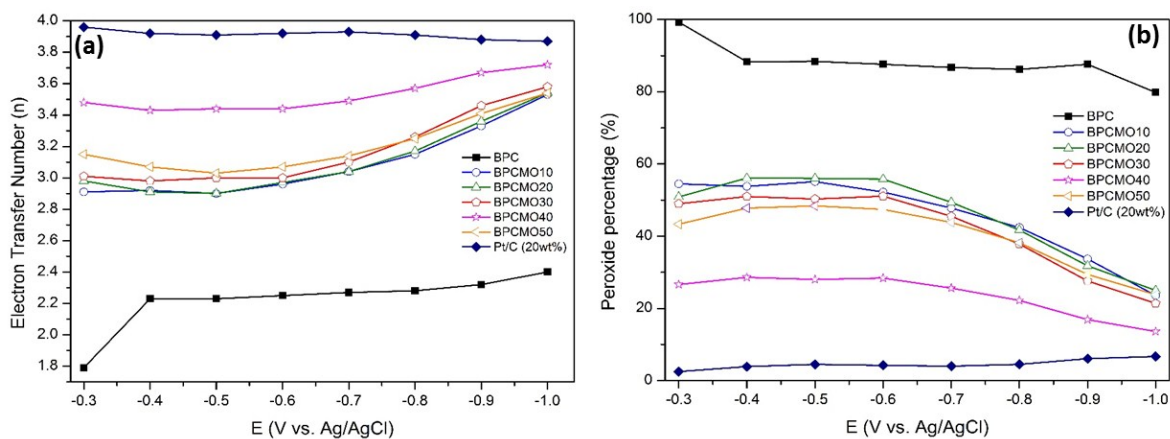


Fig. S7 (a) Electron transfer number (n) and (b) the amount of peroxide (HO_2^-) of BPCMO series, calculated from RRDE data at 2500 rpm and at a scan rate of 50 mV sec⁻¹.

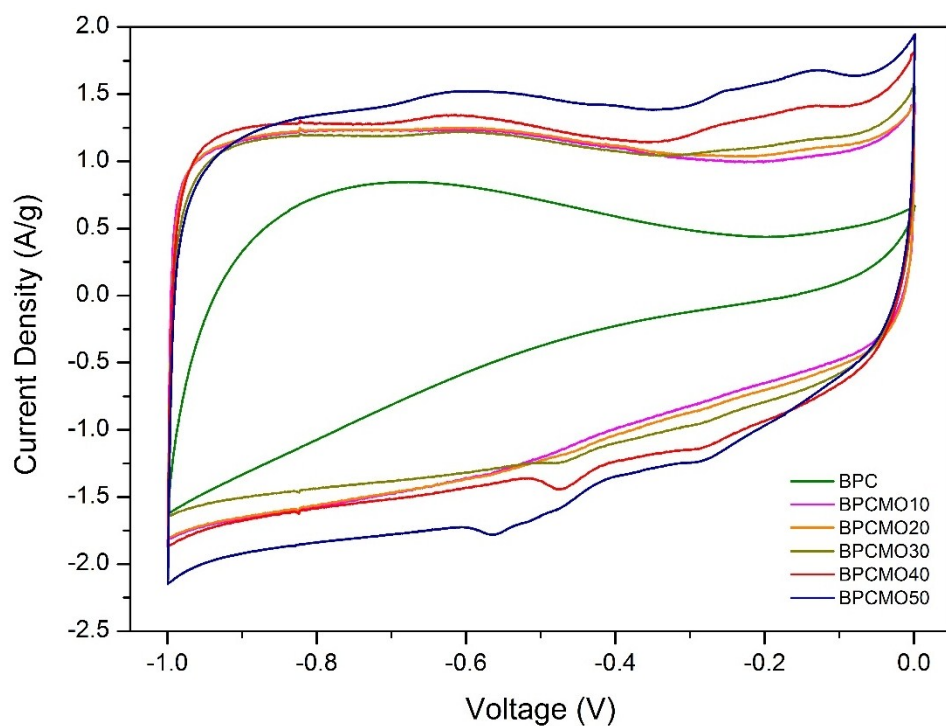


Fig. S8 CV curves of BPCMO series with potential window from -1.0 to 0.0 V at a scan rate of 10 mV sec⁻¹.

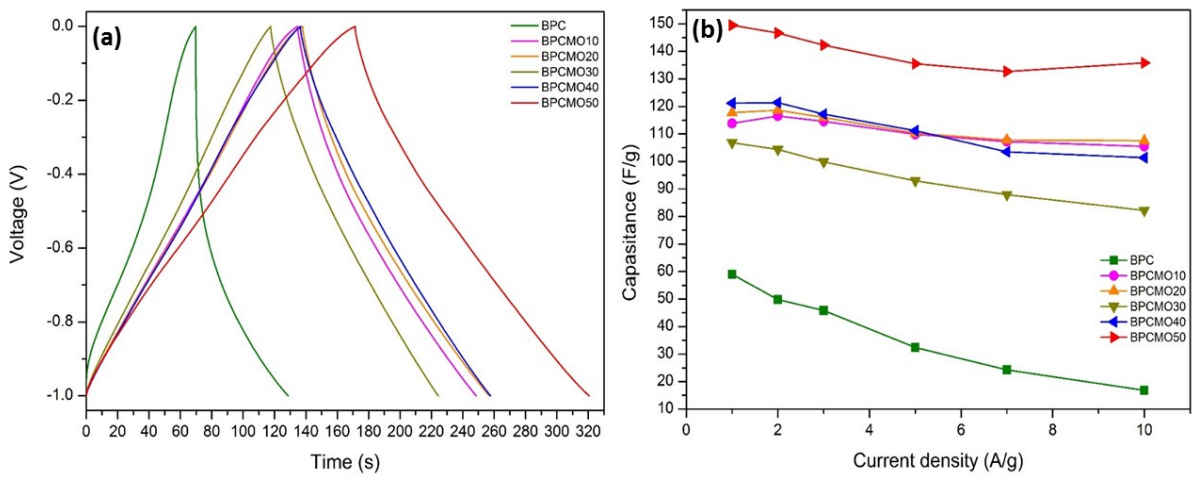


Fig. S9 Galvanostatic charge/discharge curves of BPCMO series at 1A/g in 6 M KOH and their specific capacitance at different current density.

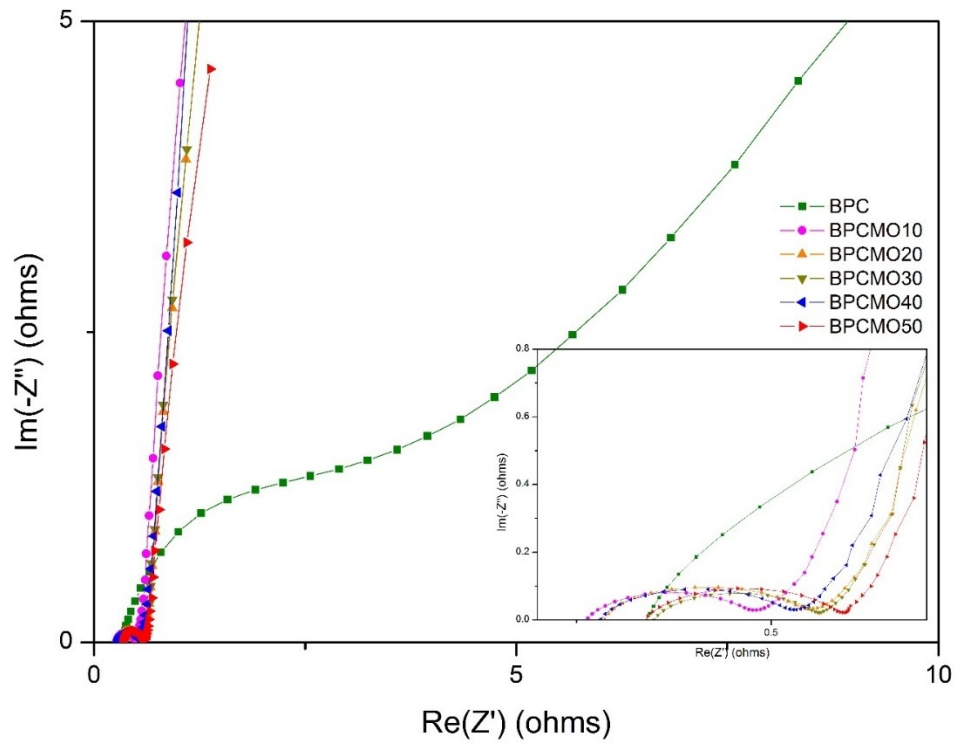


Fig. S10 Nyquist plots of BPCMO series using a sinusoidal signal of 10 mV over the frequency range from 100 kHz to 0.05 Hz.

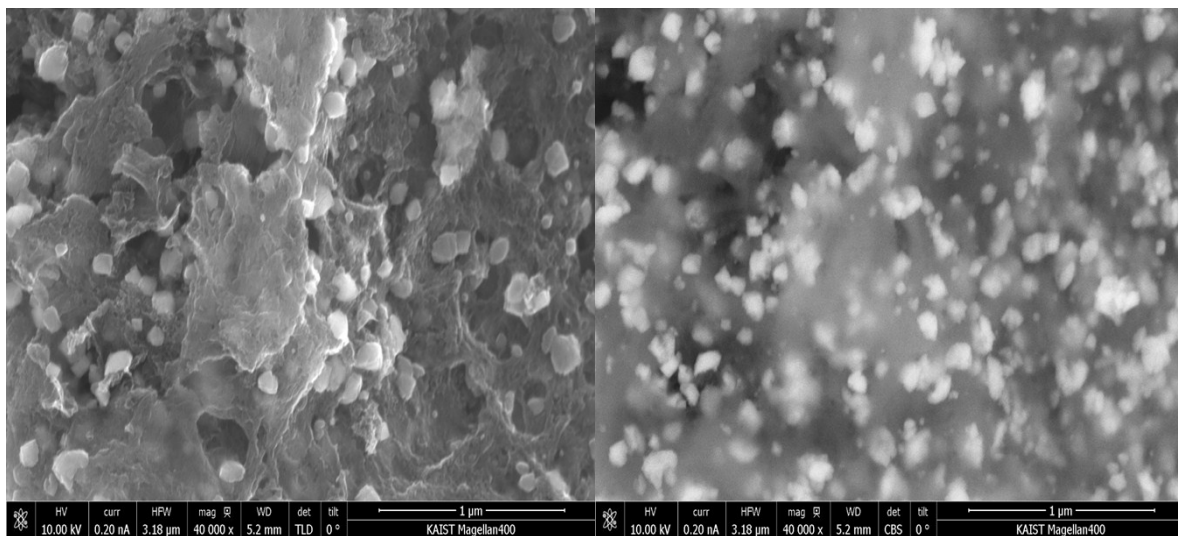


Fig. S11 SEM images of BPCMO50 after cycling test (3500 cycles) at 2 A g⁻¹.

Reference

1. Kim, G. M.; Baik, S.; Lee, J. W. Enhanced oxygen reduction from the insertion of cobalt into nitrogen-doped porous carbons. *RSC Adv.* **2015**, *5*, 87971-87980.
2. Baik, S.; Lee, J. W. Effect of boron-nitrogen bonding on oxygen reduction reaction activity of BN Co-doped activated porous carbons. *RSC Adv.* **2015**, *5*, 24661-24669.
3. Chen, S. M.; Ramachandran, R.; Mani, V.; Saraswathi, R. Recent advancements in electrode materials for the high-performance electrochemical supercapacitors: a review. *Int. J. Electrochem. Sci.* **2014**, *9*, 4072-4085.